Air Parcel Trajectories and Snowfall Related to Five Deep Drilling Locations in Antarctica Based on the ERA-15 Dataset*

C. H. REIJMER AND M. R. VAN DEN BROEKE

Institute for Marine and Atmospheric Research, Utrecht University, Utrecht, Netherlands

M. P. SCHEELE

Royal Netherlands Meteorological Institute, De Bilt, Netherlands

(Manuscript received 23 May 2001, in final form 30 November 2001)

ABSTRACT

Five-day backward air parcel trajectories are used to define potential moisture sources of snow falling at five Antarctic deep drilling locations: Byrd, DML05, Dome C, Dome F, and Vostok. The trajectory calculations are based on European Centre for Medium-Range Weather Forecasts reanalysis data, ERA-15 (1979–93). Based on model precipitation, a distinction is made between cases with and without snowfall at the point of arrival. ERA-15 precipitation is in reasonable agreement with measured accumulation at Byrd, but seriously underestimates the amount of precipitation on the East Antarctic ice sheet. The trajectories show that the oceans closest to the site contribute the most moisture. The latitude band contributing most (~30% of the total annual precipitation) is 50°–60°S, that is, the area just north of the sea-ice edge. The calculated trajectories show seasonal dependency, resulting in a seasonal cycle in the moisture sources, which is further enhanced by a seasonal cycle in the amount of precipitation. The interannual variability of the source regions is of the order of 3° latitude. At DML05, a significant northward moving moisture source region is detected, while at Dome C a significant southward movement is observed.

1. Introduction

Deep ice cores have been drilled at several locations in the Antarctic and Greenland ice sheet; for example, Vostok, Byrd, and Dome F in Antarctica; Greenland Ice Core Project (GRIP and North GRIP); and Greenland Ice Sheet Project (GISPII) (see, e.g., GRIP Members 1993; Dome-F Ice Core Research Group 1998a,b; and Petit et al. 1999). The main objective of the European Project for Ice Coring in Antarctica (EPICA) is to construct a high-resolution climate record for the Antarctic by drilling two additional cores and compare the results with other Antarctic and Greenland records. The EPICA cores are drilled at Dome C (Wolff et al. 1999) and DML05 (Oerter et al. 2000; Fig. 1). The low accumulation rate at Dome C, ~36 millimeters water equivalent per year (mmwe yr^{-1}; Petit et al. 1982), hopefully produces a record of several glacial–interglacial cycles, while the relatively high accumulation rate at DML05, ~62 mmwe yr^{-1} (Oerter et al. 2000), enables one to obtain a detailed record of the last glacial–interglacial cycle. Furthermore, DML05 is located in Dronning Maud Land (DML), an area that is considered to be an important link between Antarctic and Greenland ice core records.

The climate recorded in ice cores is determined by the conditions that prevail when snowfall occurs. These need not be representative for the mean climate conditions at that point (Noone et al. 1999). Factors such as seasonality of snowfall and changes in moisture source region may bias the ice core record in a systematic way (Jouzel et al. 1997; Schlosser 1999). Several techniques have been used to trace moisture source regions of Antarctic snow. Petit et al. (1991) and Ciais et al. (1995) use deuterium excess as tracer in combination with idealized isotope models. They conclude that the Antarctic moisture has a subtropical origin, 30°–40°S and 20°–40°S, respectively. Peixoto and Oort (1992) came to the same conclusion on the basis of atmospheric water balance studies (8°–40°S). Other studies including $\delta^{18}O$ (Bromwich and Weaver 1983), general circulation models (GCMS; Delaygue et al. 2000; Delmotte et al. 2000), and trajectory studies (Reijmer and van den Broeke 2001) suggest a more southerly origin, 55°–60°S, 30°–60°S, and 40°–60°S, respectively.

* European Project for Ice Coring in Antarctica Publication Number 42.

Corresponding email address: Dr. C. H. Reijmer, Institute for Marine and Atmospheric Research, Utrecht University, P.O. Box 80005, Utrecht 3508 TA, Netherlands.
E-mail: C.H.Reijmer@phys.uu.nl

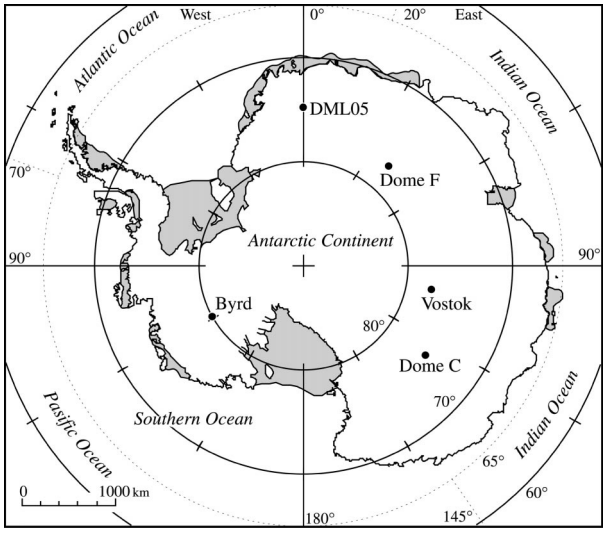

FIG. 1. Map of Antarctica showing the arrival locations of the trajectories. Dotted lines are boundaries of ocean regions defined in the text.

In this study we use a trajectory model and European Centre for Medium-Range Weather Forecasts (ECMWF) reanalysis (ERA-15) data to trace moisture sources of five Antarctic locations. The locations chosen are the two EPICA drilling sites (DML05 and Dome C) and three sites on the polar plateau where earlier deep drillings have been carried out in the past, namely Byrd, Vostok, and Dome F (Herron 1982; Legrand and Delmas 1987; Dome-F Ice Core Research Group 1998b; Fig. 1 and Table 1). The approach in this study is similar to that of Reijmer and van den Broeke (2001), who described trajectories to DML05 for 1998. Noone et al. (1999) also used ERA-15 data to describe seasonal patterns and trajectories of significant snowfall in the Dronning Maud Land region.

In section 2 the trajectory model and ERA-15 are briefly described. Section 3 describes the characteristics of the model snowfall compared to measurements. In section 4 the calculated trajectories are described, followed by a summary and discussion of the results.

2. The trajectory model

To calculate air parcel backward trajectories we use the trajectory model developed by the Royal Netherlands Meteorological Institute (KNMI; Scheele et al. 1996). This model computes the three-dimensional displacement of an air parcel during a time step Δt using an iterative scheme:

$$\mathbf{X}_{n+1} = \mathbf{X}_0 + \frac{\Delta t}{2}[\mathbf{v}(\mathbf{X}_0, t) + \mathbf{v}(\mathbf{X}_n, t + \Delta t)]. \quad (1)$$

In this equation, Δt is the iteration time step, $\mathbf{X}_0$ is the position vector of the parcel at time t, $\mathbf{X}_n$ is the nth iterative approximation of the position vector at time $t + \Delta t$, and $\mathbf{v}(\mathbf{X}, t)$ is the wind vector at position $\mathbf{X}$ and time t. The iteration time step is -10 min. The iteration stops when the horizontal distance between $\mathbf{X}_n$ and $\mathbf{X}_{n+1}$ is less than 300 m and the relative vertical (pressure) difference, defined as $(P_{n+1} - P)/P_{n+1}$, is less than 0.0001. The model is able to compute different types of trajectories, for example, isentropic, isobaric, or three-dimensional. The latter is used because it most accurately approximates the true three-dimensional transport path (Stohl et al. 1995; Kottmeier and Fay 1998).

As input for the trajectory model we use ERA-15 data (1979–93; Gibson et al. 1997). To ensure physical balance in the meteorological fields the 6-h forecasted wind fields are used, not the analysed wind fields, giving the most accurate representation of the vertical wind speed component. ERA-15 data have a horizontal spectral resolution of T106 (~1.7°) and 31 σ-levels in the vertical. For the trajectory model, the resolution of the input data is kept constant at 1.5° in the horizontal plane, 31 levels in the vertical, and 6 h in time. This makes interpolation in time and space necessary: spatial interpolation is bilinear in the horizontal, linear in the

TABLE 1. Characteristics of the five starting points for the backwood trajectory calculations (Fig. 1). Elevation is measured elevation, and ERA-15 model elevation is in parentheses; P is model precipitation; Acc. is measured accumulation. The surface slope and distance from the coast are based on a 10 km by 10 km Antarctic topography (data courtesy of J. Bamber, Bristol University). The error estimate in the model precipitation is that standard deviation in the annual means over the 15-yr period.

Station	Lat	Lon	Elev (m ASL)	Slope (m km^{-1})	Distance (km)	P (mmwe yr^{-1})	Acc.
Byrd	80°0′S	119°24′W	1530 (1605)	3.5	689.5	159 ± 53	160[a]
DML05	75°00.2′S	0°00.4′E	2892 (2769)	1.3	602.0	29 ± 6	62 ± 21[b]
Dome C	74°30′S	123°0′E	3280 (3042)	0.3	945.4	16 ± 9	36 ± 5[c]
Dome F	77°19′S	39°42.2′E	3810 (3283)	0.0	927.8	7 ± 3	30[d]
Vostok	78°30′S	106°54′E	3488 (3409)	1.0	1362.5	6 ± 2	22.5[e]

[a] Herron (1982).
[b] Oerter et al. (2000).
[c] Petit et al. (1982).
[d] Dome-F Ice Core Research Group (1998b).
[e] Legrand and Delmast (1987).

logarithmic value of the air pressure in the vertical, and the time interpolation is quadratic (Scheele et al. 1996).

Uncertainties that are introduced by the choice of trajectory type, interpolation schemes, and temporal and spatial resolution of the input wind fields are on the order of 1000 km after 5 days calculation (Kahl et al. 1989; Doty and Perkey 1993; Stohl et al. 1995). In reality, the uncertainty is even larger because of the difference between the forecasted wind fields and the real winds and the presence of convective systems (such as fronts). In a convective system the air parcel loses its identity making it impossible to truly trace a single parcel. Fortunately, precipitation in the continental polar atmosphere is generally stratiform and convective mixing is usually insignificant. Kahl et al. (1989) conclude that sensitivity due to differences in gridded meteorological databases—that is, the input wind fields, an indicator for errors in the wind fields—can be larger than the sensitivity due to different trajectory calculation methods. These important sources of errors in trajectories are difficult to assess and are not quantified in the uncertainty estimates presented by, for example, Kahl et al. (1989). The above implies that the identified source regions after 5 days have an uncertainty of more than ~10° latitude.

An additional problem that influences the wind fields in the ERA-15 dataset is the Antarctic orography used in the model. Genthon and Braun (1995) show that the ERA-15 orography is up to 1000 m too high in western DML and up to 1000 m too low in eastern DML. Additionally Bromwich et al. (2000) show that a faulty elevation of Vostok station leads to important errors in the ERA-15 atmospheric circulation. These systematic errors affect flow patterns over a large part of the East Antarctic ice sheet and to a lesser extent over the West Antarctic ice sheet. However, Cullather et al. (1997) showed that the analyses, and therefore probably also the forecast fields in ERA-15, are superior to analyses of the National Centers for Environmental Prediction for large-scale circulation features and moisture budget of the high southern latitudes. A final problem using the trajectory method is the fact that not the moisture itself but an air parcel containing moisture is traced, which complicates the position-finding of the region where moisture actually enters the air parcel. Possible replacement of moisture through cycles of condensation and evaporation is not taken into account. We nevertheless think that the computed trajectories give a reasonable estimate of the source regions of Antarctic moisture and the assumption is made that the main moisture source of Antarctic precipitation is distributed along the 5-day trajectories.

Trajectory calculations are initiated (and air parcels arrive) every 12 h (0000 UTC and 1200 UTC) at six different pressure levels above the surface. Table 2 presents these six levels and the mean model surface pressure at the five locations. The lowest three to four levels are reasonably close to the surface in the layer with maximum poleward moisture transport (Noone et al. 1999). The higher levels represent the large-scale flow. Trajectories that intersect with the surface are omitted from the analysis; this represents ~10% of the trajectories starting at the lowest level.

TABLE 2. Starting pressure levels for the air parcel backward trajectory calculations and mean surface pressure (P_0), in hPa.

Level	Byrd	DML05	Dome C	Dome F	Vostok
Surface (P_0)	805.9	685.6	661.3	639.7	630.9
1	800	680	650	630	620
2	790	670	640	620	610
3	780	660	630	610	600
4	750	625	600	575	575
5	700	575	550	525	525
6	625	500	475	450	450

In the following a distinction is made between trajectories with and without snowfall on arrival at the sites based on ERA-15 snowfall. ERA-15 snowfall is based on the cumulative snowfall in the first 12 forecast hours and suffers from model spinup, and is ~9% less than the amount from the 12- to 24-h forecast (Turner et al. 1999). To mark a trajectory as a snowfall trajectory, unless stated otherwise, at least 1.0, 0.35, 0.25, 0.20, and 0.15 mmwe of snow must have accumulated in the 12 h preceding the parcel arrival at Byrd, DML05, Dome C, Dome F, and Vostok, respectively. This ensures that ~50% of the total model precipitation is represented in the snowfall trajectories. Unless stated otherwise, all events refer to amount of precipitation in 12 h.

3. Precipitation

The main mechanisms leading to precipitation in the coastal regions and on the East Antarctic plateau are described by, for example, Bromwich (1988), King and Turner (1997), and Cullather et al. (1998). Precipitation in the coastal areas of Antarctica is often orographically induced. The cyclones associated with the snowfall in the coastal regions seldom penetrate far inland and precipitation over the higher parts of the Antarctic plateau, where Dome F, Vostok, and Dome C are located, may also be associated with radiative cooling of the air, instead of orographic lifting (Bromwich 1988). The precipitation amounts on the plateau are usually small.

Owing to the orographic nature of most Antarctic precipitation, errors in the model orography can have great influence on the amount and location of model snowfall. This complicates the comparison between measured and modeled accumulation, and will have the largest effect on the amount of precipitation at the stations reasonably close to the coast, DML05 and Byrd. Genthon and Braun (1995) show that the ERA-15 orography is up to 1000 m too high in western DML resulting in too little precipitation on the Antarctic plateau in this area (Turner et al. 1999), and up to 1000 m too low in eastern DML where Dome F is located. Table 1 shows

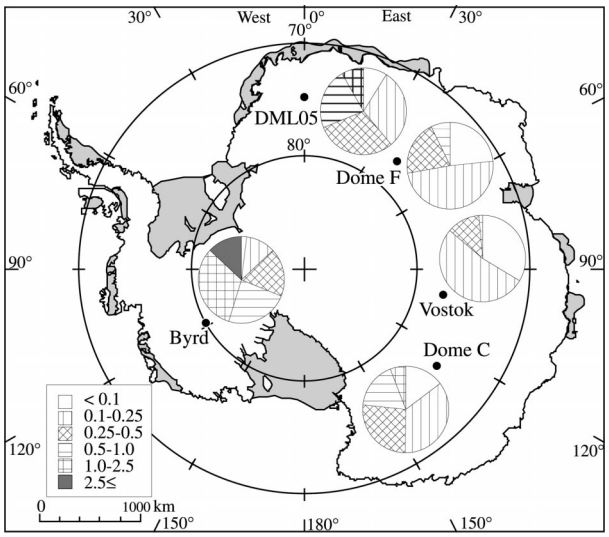

FIG. 2. Percentage of the total 15-yr precipitation at the five sites grouped by 12-hourly totals bound by <0.1, 0.25, 0.5, 1.0, 2.5, and ≥2.5 mmwe (12 h)$^{-1}$.

that at all stations, except Byrd, the model orography is too low, from 79 m at Vostok to 527 m at Dome F. Other factors complicating the comparison between measured accumulation and modeled precipitation, is the model resolution and the fact that accumulation is the result of precipitation, snowdrift erosion and deposition, sublimation, and condensation. The latter processes are disregarded in the analysis, although they are probably locally not negligible (Bromwich 1988; van den Broeke 1997; Cullather et al. 1998).

Table 1 additionally presents the annual mean precipitation in ERA-15 at the five drilling locations. The precipitation decreases with increasing elevation and is exceptionally low over the East Antarctic plateau. The precipitation at Byrd is high compared to other locations. Except at Byrd, the modeled precipitation is lower than the measured accumulation presented in the literature, the difference being largest for Dome F and Vostok and in agreement with Turner et al. (1999). They compared annual mean accumulation (precipitation minus evaporation) in ERA-15 with an accumulation distribution compiled from measurements, presented by Giovinetto and Bentley (1985). Turner et al. (1999) show that on West Antarctica, ERA-15 accumulation resembles the measured accumulation while on East Antartica the model consistently underestimates precipitation. The underestimation could be due to an underestimation of clear sky precipitation. However, due to the small amount of precipitation associated with clear-sky precipitation a more likely explanation is an underestimation of the frequency and intensity of major snowfall events in the model.

Figure 2 presents the magnitude distribution of precipitation events based on 12-hourly totals. As expected from the described precipitation mechanisms and annual mean temperatures, the contribution of smaller events increases with increasing elevation and distance from the coast. At Vostok and Dome F, all events are smaller than 1 mmwe, while at Byrd ~45% of the total precipitation is caused by events larger than 1 mmwe. Dome C is slightly more continental than DML05, given the fact that ~50% of the precipitation is derived from events smaller than 0.25 mmwe at Dome C compared to ~38% at DML05. Vostok is the most continental station, with ~86% of the total precipitation caused by events smaller than 0.25 mmwe. Annual distributions (not shown) are similar to the 15-yr distribution in Fig. 2. The largest events do not occur each year and contribute significantly to the interannual variability in precipitation. The smallest events (<0.1 mmwe) contribute an equal amount at all stations each year (~2.5 mmwe).

In the model, the precipitation is mainly defined by a large number of small events, while in reality the precipitation is dominated by several major events (Fig. 3). Measurements with a sonic altimeter at DML05 (Fig. 3b) show that ~40% of the annual accumulation was deposited in ~35 events of 10 mmwe (~0.03 m of snow) per year. Events in which ~0.06 m of snow accumulates in 12 h occur ~6 times per year and contribute ~20% to the total accumulation. The occurrence

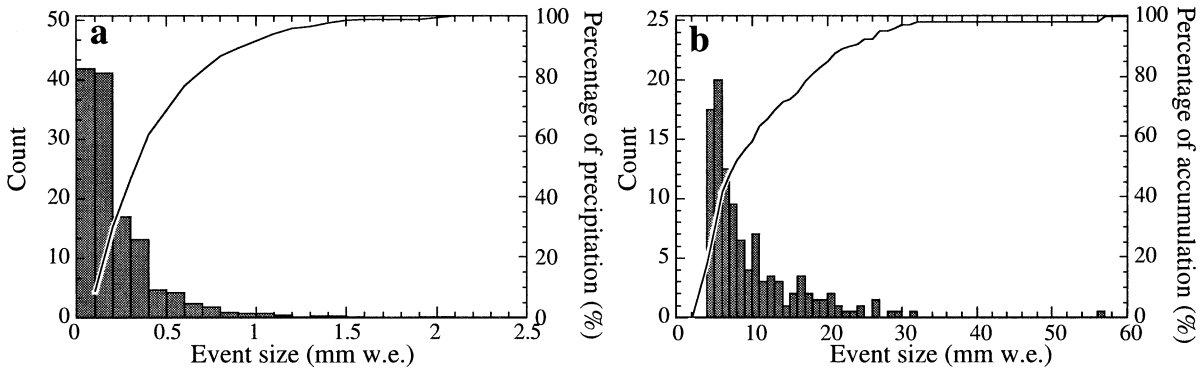

FIG. 3. Mean annual number of events per event size (left scale, bars) and percentage of annual mean precipitation contributed by events of different size (right scale, line) in (a) ERA-15 and (b) measurements at DML05.

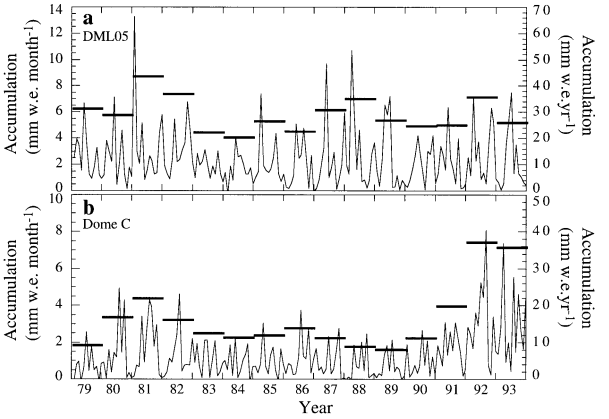

FIG. 4. Monthly and annual averaged accumulation at (a) DML05 and (b) Dome C over the ERA-15 period. Thin solid lines are monthly totals (left axis) and thick solid lines are the annual totals (right axis).

of several large events instead of many small events in the measurements suggests that the intensity of the larger events is underestimated in the model and not all small events in the model are realistic. This is the reason to take only the larger events into account in the trajectory analysis.

Figure 4 presents total annual and monthly precipitation at DML05 and Dome C for the ERA-15 period. The variability, presented as the standard deviation in the 15-yr annual mean (Table 1), is considerable. At Dome C the interannual variability is ~50% of the annual mean precipitation. The annual time series are not well correlated. Except for the correlation between Dome C and Vostok, which is 0.75, the correlation coefficients are smaller than 0.45 and not significant at the 5% level. On shorter timescales, the records are not well-correlated either. Correlation between separate events is only significant between Dome C and Vostok. The precipitation at Vostok appears to lag 0 to 12 h behind Dome C, with a maximum correlation of 0.35 at 0-h time shift. The lack of correlation between any of the other stations is probably caused by the considerable distance between the stations: >1000 km compared to ~600 km between Dome C and Vostok.

Figure 5 presents the mean annual cycle in precipitation for DML05 and Dome C. All stations show an increase in precipitation in the winter months. This was also found in measurements (Bromwich 1988) and model results (Cullather et al. 1998; Delaygue et al. 2000). The seasonal cycles at Dome F and Dome C are very similar and show a maximum in July. At DML05 and Byrd a maximum is found in May. Seasonally averaged, most precipitation at DML05 occurs in autumn (37%) and at Dome C and Dome F in winter (37% and 35%, respectively). At Vostok, most precipitation occurs in the summer months (30%) and at Byrd, precipitation is highest in autumn and winter (33% and 30%, respectively).

4. Results of trajectory calculations

a. Mean trajectories

Figure 6a presents the mean of all trajectories and Fig. 6b the mean of the snowfall trajectories, averaged over the ERA-15 period, at six different pressure levels (Table 2). Means are calculated by averaging the positions of the trajectories per time step over a sphere. All trajectories show a cyclonic curvature reflecting the substantial influence of cyclones on the air parcel paths over Antarctica. The radius of curvature is smallest for the stations closest to the coast, Byrd and DML05, where cyclonic influences are largest. The radius of curvature increases with increasing arrival altitude due to the increase in advection speed. The lower trajectories arriving at Dome F, Vostok, and Dome C mostly remain over the continent, while at Byrd and DML05 most air parcels partly travel over the ocean. Due to the higher wind speeds at higher altitudes, the distance travelled by air parcels arriving at higher altitudes is larger, at level 6 about twice as large as at level 1, and their origin is farther north and west. At Vostok and Dome C, the lower levels have more western pathways compared to

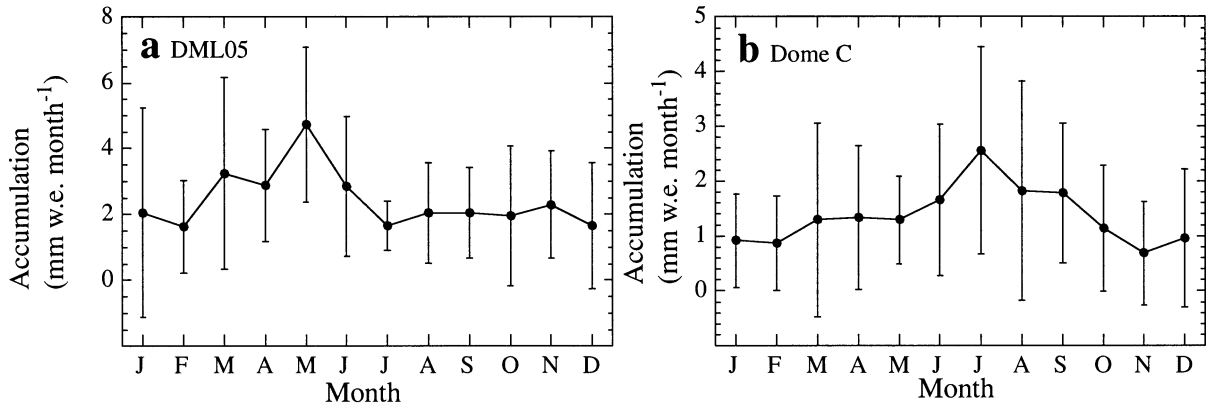

FIG. 5. Annual cycle in model precipitation based on monthly averages for (a) DML05 and (b) Dome C. The error bars denote the std dev in the 15-yr mean.

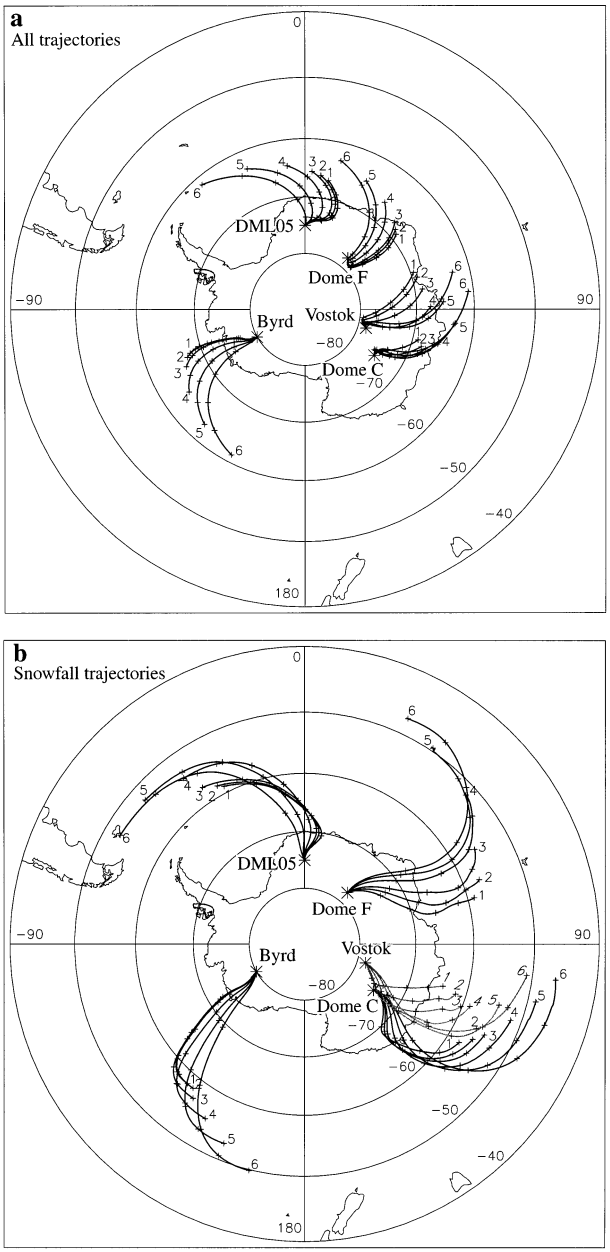

FIG. 6. Mean 5-day backward trajectories starting at six different pressure levels above the surface (Table 2; highest level is 6). Each day back is marked with a plus sign and the asterisks denote the arrival locations: (a) the mean of all trajectories and (b) the mean of the snowfall trajectories. In (b) the trajectories arriving at Vostok are gray with italic labels to distinguish them from the Dome C trajectories.

the higher levels, while at the other stations the pathways are more western with increasing altitude. Especially the pathways of the lower trajectories are influenced by the surface, which results in an abrupt anticyclonic turn in the last day before arrival. The arrival directions are mainly from the northeast at DML05 and Byrd, and south to southwest at Dome F, Dome C, and Vostok. This corresponds to the dominant wind direction near the surface at these locations, which is determined by the direction of the katabatic flow.

The snowfall trajectories presented in Fig. 6b are clearly different and originate from locations farther north. The mean distance travelled by a snowfall air parcel is about twice as large compared to nonsnowfall air parcels (~3500 km vs ~1750 km). At Byrd and DML05, the trajectories also originate from farther west. At Dome F, Vostok, and Dome C, the trajectories are shifted to the east when compared to the mean of all trajectories. The resulting trajectories arriving at Vostok show that the air parcels travelled over Dome C before arrival and originate from about the same region. This could partly explain the correlation between precipitation at Dome C and Vostok. However, the overlap and correlation could also be due to the faulty station elevation of Vostok in the model, resulting in a systematic error in the atmospheric circulation in this area.

The different nature of the snowfall trajectories is further illustrated in Fig. 7, which presents pressure and equivalent potential temperature θ_e along the average trajectories arriving at DML05, at 625 hPa (level 4), the level closest to the maximum in poleward moisture transport, ~60 hPa above the surface (Noone et al. 1999). Results for the other locations are similar. Figure 7a shows that on average snowfall trajectories are situated at higher pressure levels and have higher surface pressure along their path, which means that snowfall trajectories travel closer to the surface and closer to sea level. Air parcels in snowfall trajectories are therefore more likely to interact with the surface. However, the exact location of moisture uptake is difficult to asses. The figure does not show whether the parcels are in the boundary layer and whether surface evaporation occurs.

Figure 7b presents θ_e, the temperature a parcel would have when brought adiabatically to 1000 hPa with all its moisture condensed and the resulting latent heat used to warm the parcel. The figure shows that snowfall trajectories are relatively warm and moist compared to all trajectories. Their temperature (not shown) is 10° to 15°C higher and remains fairly constant until the continent is reached, ~1 day before arrival. The specific humidity for the snowfall trajectories (not shown) is also fairly constant until the continent is reached with a small maximum ~4 days before arrival. The mean specific humidity for all trajectories is much lower owing to the lower temperature, and decreases in a linear fashion. Seasonally (not shown) the small maximum in specific humidity varies between 3 days before arrival in summer to 5 days in autumn.

The above suggests that snowfall trajectories best describe the moisture transport to Antarctica. Therefore, in the remaining part of this paper only results from snowfall trajectories are described. Parcels arriving at level 4 are taken to represent the largest moisture transport. The maximum in specific humidity 3 to 5 days before arrival and the proximity of the sea surface in

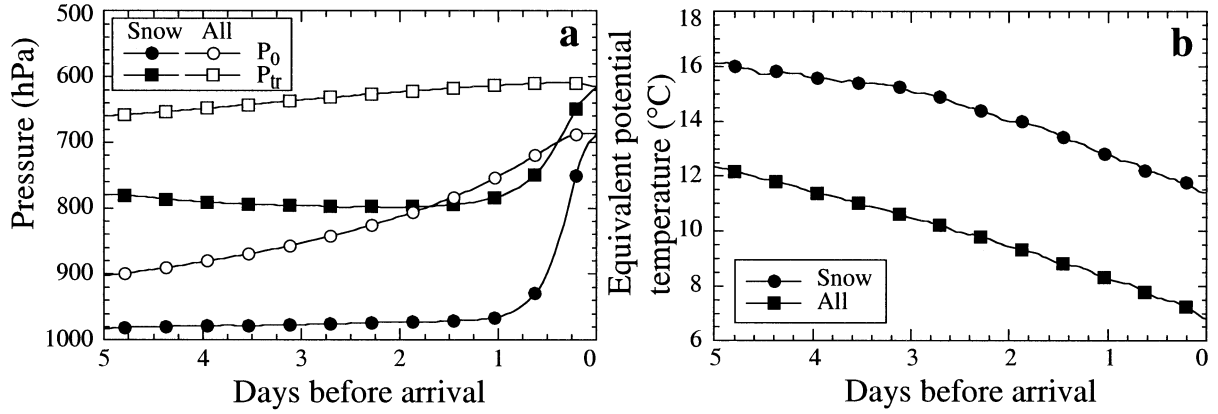

FIG. 7. (a) Mean pressure, (b) equivalent potential temperature of snowfall and all trajectories arriving at DML05 at 625 hPa (level 4); P_0 is surface pressure (squares) and P_{tr} is trajectory pressure (dots).

that time suggests that the origin of the moisture lies 3 or more days before arrival. Reijmer and van den Broeke (2001) show for an individual snowfall event that only ~5% of the moisture precipitating at DML05 originates more the 5 days before arrival and ~50% originates ~3 to 5 days before arrival. On a 15-yr average the amount of moisture originating more than 5 days before arrival is larger although a small maximum in specific humidity does occur ~4 days before arrival. The location of the air parcels 4 days before arrival will therefore be taken as representative for the main potential source region for moisture.

Judging from the general cyclonic curvature of the trajectories, the air parcel paths are likely to be influenced by the seasonality in strength and location of cyclones. However, Reijmer and van den Broeke (2001) did not find a clear annual cycle for 1998. This could be due to the short time period, while 5 to 10 years of precipitation data are necessary to obtain a significant seasonal cycle in precipitation. Figure 8 shows seasonally averaged snowfall trajectories. In summer [December–January–February (DJF)] when cyclones are less intense and travel at farther distance from the continent, the cyclonic curvature of the trajectories is small and the air parcels have their most southern and eastern origin. In the autumn and spring [March–April–May (MAM) and September–October–November (SON)], when the surface pressure shows a minimum and cyclones are most intense and travel closest to the continent, the trajectories show their most western origin and air parcels travel the largest distances. Winter [June–July–August (JJA)] trajectories are similar to autumn and spring, but have a slightly more northern origin. At Byrd, the seasonal shift is smallest, while at Vostok the seasonal shift is largest. Here, the cyclonic curvature is entirely absent in summer.

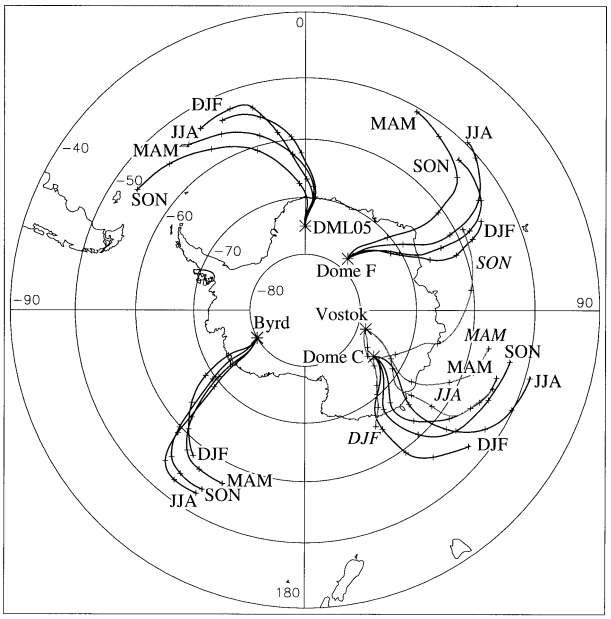

FIG. 8. Mean 5-day backward trajectories arriving at level 4 above the surface. Different seasons are denoted by DJF (summer), MAM (autumn), JJA (winter), and SON (spring). Trajectories arriving at Vostok are gray with italic labels to distinguish them from the Dome C trajectories.

Assuming that the moisture source of Antarctic precipitation lies somewhere along the 5-day mean snowfall trajectory, we speculate that the moisture sources for the precipitation is located between 50° and 60°S for all five locations. At DML05 the moisture originates probably from the western part of the South Atlantic Ocean in agreement with Reijmer and van den Broeke (2001). At Dome F, Vostok, and Dome C, the Indian Ocean provides the moisture. The source region of Vostok and Dome C precipitation is at almost the same location, in the eastern part of the Indian Ocean. Precipitation at Byrd comes from the Pacific Ocean.

b. Moisture source regions

To get a better insight in the actual contribution of the various oceans and latitude bands to the precipitation

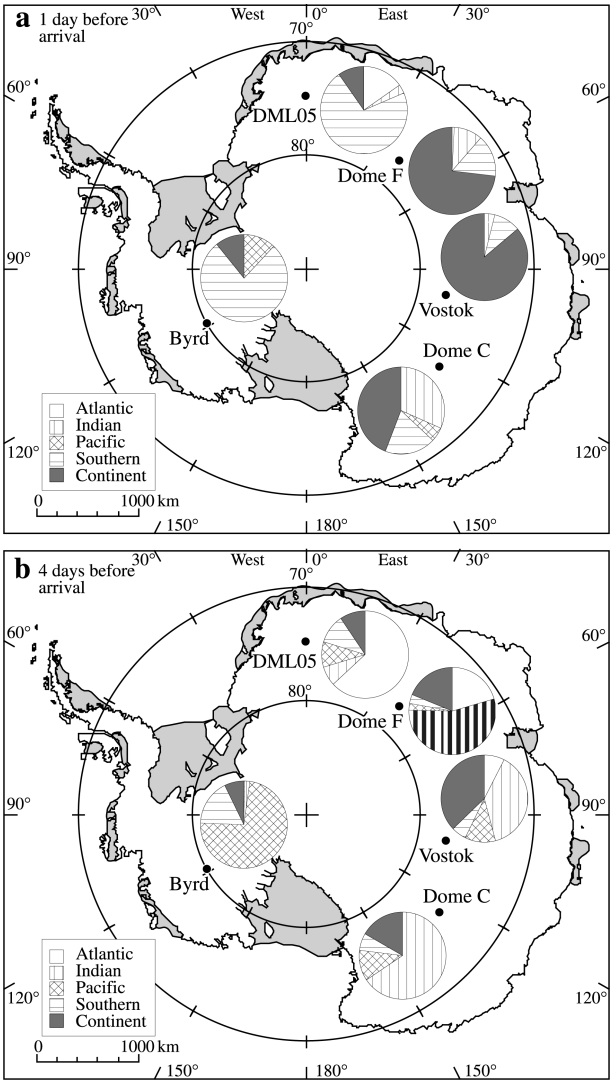

FIG. 9. Percentage of the snowfall trajectories arriving at level 4 distributed over the five ocean regions, for days (a) 1 and (b) 4 before arrival. Ocean regions are defined in the text and in Fig. 1.

at the five drilling sites, the Southern Hemisphere is divided in five regions similar to the regions presented by Reijmer and van den Broeke (2001): the southern Atlantic Ocean (70°W–20°E), the southern Indian Ocean (20°–145°E), the southern Pacific Ocean (145°E–70°W), the Southern Ocean (between the Antarctic continental boundaries and 65°S), and the Antarctic continent (Fig. 1). Furthermore, the Southern Hemisphere is divided into six latitude bands bound by 40°, 50°, 60°, 70°, 80°, and 90°S. Figure 9 presents the percentage of the snowfall trajectories distributed over the five ocean regions 1 and 4 days before arrival. The air parcels arrive at level 4 (Table 2).

Figure 9a shows that 1 day before arrival at Dome F, Vostok, and Dome C, most air parcels (45%–85%) are above the Antarctic continent. At DML05 and Byrd, which are located closer to the coast, more than 50% of the snowfall trajectories are still over the Southern Ocean. From days 2 to 5, the contribution of the continent and Southern Ocean decreases and the contribution of the ocean closest to the station increases. The larger the distance from the coast, the larger the amount of trajectories that remain over the Southern Ocean or continent. The main moisture contributor for DML is the Atlantic Ocean, with ~60% of the trajectories located there 3 to 5 days before arrival. Due to the cyclonic curvature of the trajectories, the contribution of the Pacific Ocean increases with increasing time before arrival at DML05, to 10% at day 5. The contribution of the Indian Ocean is ~7%. These results are similar to the results presented by Reijmer and van den Broeke (2001) for 1998, and to the present-day climate simulation of Delaygue et al. (2000), although the contribution of the Pacific Ocean is larger in the latter and smaller in the former. At Dome F, the contribution of the Indian Ocean dominates, and varies between 45% and 65%. The contribution of the Atlantic Ocean is ~25%. The influence of the Pacific Ocean on Dome F is negligible. At Vostok, the contribution of the Atlantic Ocean is ~7%, and is of the same magnitude as the contribution of the Pacific Ocean. The main contributor of moisture to the snowfall at Vostok is the Indian Ocean (30%–45%), and the contribution of the continent remains larger than 25%. In comparison, Delaygue et al. (2000) show a contribution of the continent of less than 10% to the precipitation at Vostok. In their study, the Indian Ocean is also the main contributor, but the contribution of the Indian Ocean as well as the Atlantic and Pacific Ocean is higher. At Dome C, the contribution of the Atlantic Ocean is negligible. About 60%–75% of the snowfall originates from the Indian Ocean. Although located reasonably close to the Pacific Ocean, the contribution of the Pacific Ocean is only 8% to 15%, due to the cyclonic curvature of the trajectories. The main moisture source for Byrd is the Pacific Ocean (65%–75%). The contribution of the Indian Ocean to the precipitation at Byrd is surprisingly small, ~5%. The contribution of the Atlantic Ocean is negligible. The small influence of the Indian Ocean on Byrd is caused by the small curvature in the mean snowfall trajectories.

Figure 10 presents the percentage of precipitation of which the trajectories are located in six latitude bands, 4 days before arrival. The air parcels arrive at level 4 (Table 2). The contribution of different latitude bands to the precipitation is very similar for all stations. A maximum contribution of ~30% is found between 50° and 60°S. About 75% is contributed by the latitude band 40°–70°S. Less than 10% originates from north of 40°S. At Vostok and to a lesser extend at Byrd, the maximum is located closer to the continent, between 70° and 80°S for Vostok and 60°–70°S for Byrd. This suggests a considerable contribution of the Southern Ocean to the precipitation at Vostok. However, the systematic error in the atmospheric circulation for Vostok and to a lesser extend Dome C (Bromwich et al. 2000) could influence

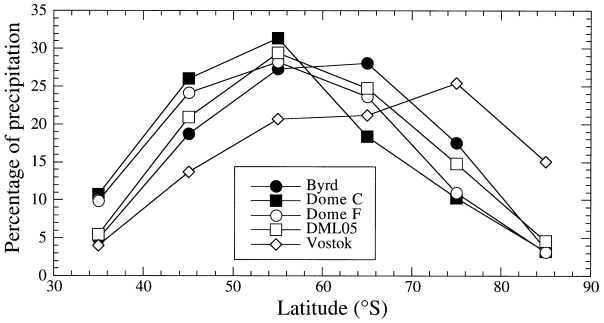

FIG. 10. Percentage of precipitation for which the trajectories are located in six latitude bands, bounded by 40°, 50°, 60°, 70°, 80°, and 90°S 4 days before arrival at level 4.

these results. The ocean regions are not very sensitive to this error due to the general cyclonic curvature of the trajectories and the location of the stations in the eastern sector of the Indian Ocean. Different advection speeds could, however, change the latitude region from which the parcels originate.

We briefly looked at seasonal cycles in the ocean and latitudinal distribution. Figure 11 presents the ocean and latitude distribution per season for DML05 and Dome C. In winter, the trajectories have their most northern origin, which is reflected in the largest contribution of the ocean closest to the stations in this season (Figs. 11a,b). The radius of curvature is smallest in the equinoctial seasons at all stations, which results in the largest contribution of the ocean west of the closest ocean in these seasons, for example, Pacific Ocean at DML05 and Atlantic Ocean at Dome F. At Dome C, the contribution of the Indian Ocean is smallest and that of the Pacific Ocean is largest in summer. At Vostok the contribution of the Indian and Pacific Ocean are similar in summer, while in the other months the Indian Ocean dominates (not shown). At Byrd, the east–west differences are small and seasonality is most pronounced in latitude distribution.

Figure 11c shows that there is no significant seasonality in the latitude distribution of the potential moisture sources of DML05. The maximum is always between 50° and 60°S. The magnitude of the maximum is largest in autumn when most precipitation occurs. The contribution to the total precipitation of this season and latitude band is ~12%. At Dome F, the maximum is located most northerly in autumn and winter, and moves south in spring and summer. Because most snow at Dome F falls in winter, this maximum at low latitudes in summer has only a small effect on the annual distribution (Fig. 10). The distribution at Vostok is similar to Dome F. In winter and spring most moisture originates from 50°–

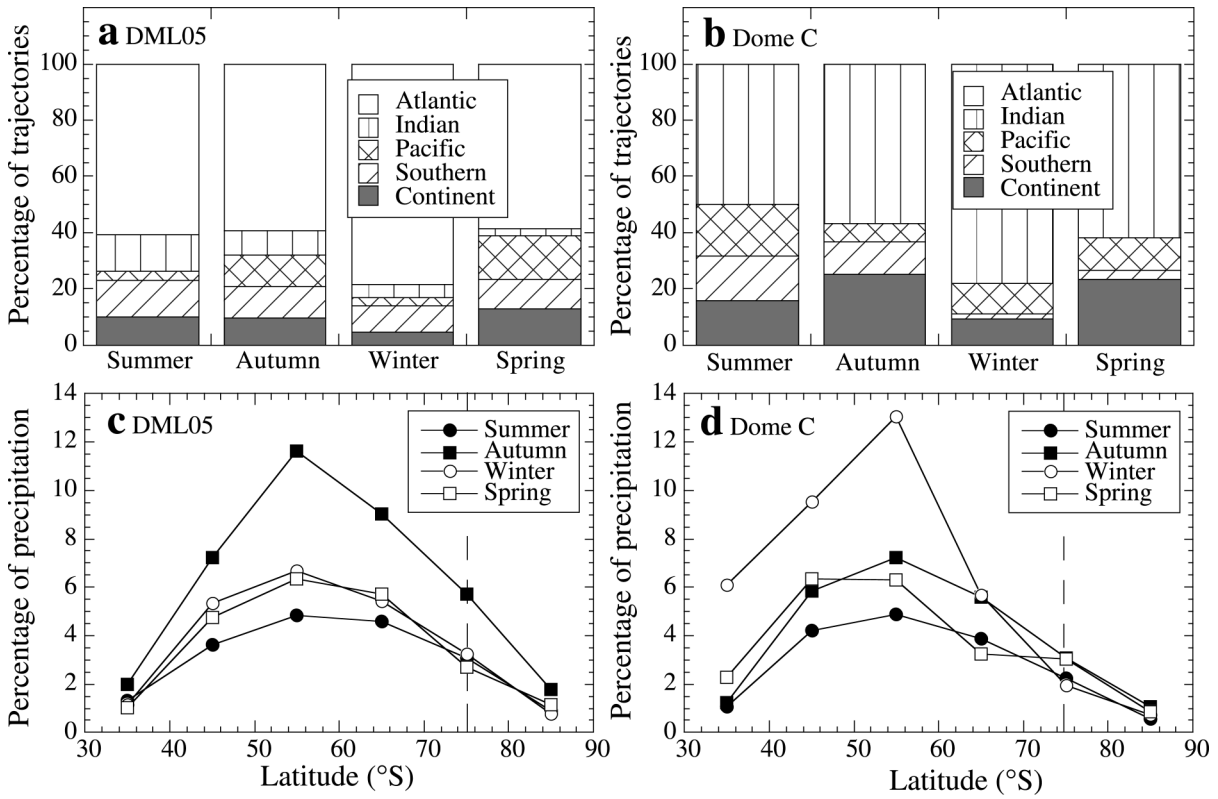

FIG. 11. Percentage of the snowfall trajectories distributed over the (a), (b) ocean regions and (c), (d) latitude bands per season. The regions are defined in the text. The location is taken 4 days before arrival at level 4 at (a), (c) DML05 and (b), (d) Dome C. Dashed lines indicate the latitude location of the stations.

60°S, in summer from south of 70°S. Because the precipitation is fairly evenly distributed over the seasons at Vostok, the shift south of the moisture origin is clearly visible in the annual distribution (Fig. 10). The distribution at Dome C is similar to Dome F and Vostok, although the maximum shift south occurs in autumn (Fig. 11d). Almost half of the annual 55% from band 40°–60°S at Dome C is contributed in winter. At Byrd, the location of the source region is most south in summer and most north in winter. The maximum contribution occurs in autumn and winter from latitude band 50°–70°S.

c. Interannual variability

Figure 12 presents the annual mean latitude location of the air parcels 4 days before arrival at level 4 for DML05 and Dome C. The average location is at ~60°S for all stations, except Vostok. The interannual variability expressed in the standard deviation in the 15-yr mean increases with increasing distance from the coast of the arrival location from 2.0 at DML05 to 4.9 at Vostok. For individual years, temporal variability is larger when the average location is located more to the south. For example, the standard deviation in the annual mean increases in a linear fashion from 2.0 to 3.0 when the average location for DML05 moves from 58° to 66°S. In the 15-yr ERA period, there is a trend northward of this region for all stations except Dome C. The trend is, however, only significant at the 5% level at DML05. At Dome C there is a significant trend southward. There is no clear explanation for this trend.

Except at Vostok, a southward migration of the average location goes together with an eastward migration. The interannual variability in longitude location is considerable (Figs. 12c,d) and is of the same order of magnitude as the seasonal variability. The standard deviation in the 15-yr mean is 9.9 at DML05 and 4.9 at Dome C. There is no significant trend at any of the stations. The large variability can result in a shift in main ocean contribution. At Vostok the shift is largest and varies from the Atlantic Ocean in 1982 to the Pacific in 1987 and 1991 (not shown).

The location of the parcels is an intricate function of the strength and tracks of cyclones, and is therefore related to the annual mean precipitation, temperature, and pressure. In general, at DML05, Dome F, and Dome C this relation results in a potential moisture source region located more south in years with high annual mean temperature, high surface pressure, and high precipitation, while at Vostok and Byrd the potential source regions are located more south in years with less precipitation and lower surface pressure and temperature.

5. Summary

Potential moisture source regions for snow falling at five locations on Antarctica were determined using 5-day backward air parcel trajectories based on the European Centre for Medium-Range Weather Forecasts 15-yr reanalysis data (ERA-15). Five ice core drilling sites (Byrd, DML05, Dome C, Dome F, and Vostok) were chosen as arrival points. A distinction is made between trajectories with and without snowfall at arrival, based on model precipitation. Trajectories were marked as snowfall trajectories when at least 1.0, 0.35, 0.25, 0.20, and 0.15 mmwe of snow accumulated in the 12 h preceding the parcel arrival at Byrd, DML05, Dome C, Dome F, and Vostok, respectively, ensuring that ~50% of the total annual model precipitation is represented in the snowfall trajectories.

The model precipitation at Byrd is in reasonable agreement with measured accumulation, but on the East Antarctic ice sheet, where the other sites are located, the model seriously underestimates precipitation, probably due to an underestimation of the frequency and especially intensity of major snowfall events in the model as shown by measurements. Another explanation could be the underestimation of clear sky precipitation in the model. The underestimation of precipitation over the East Antarctic plateau results in a representation in the snowfall trajectories of only ~25% of the total measured accumulation. However, when most of the underestimation is explained by an underestimation of snowfall intensity most snowfall events are represented in the analysis, which will give a reasonable estimate of potential source region. Averaged over the 15-yr period, the model precipitation shows a seasonal cycle. Peaks are found at DML05 and Byrd in autumn, at Dome C and Dome F in winter and at Vostok in summer. However, the temporal variability is considerable.

The mean trajectories show a cyclonic curvature reflecting the substantial influence of cyclones on air parcel pathways over Antarctica. Snowfall trajectories are about twice as long as nonsnowfall trajectories and originate generally from farther north and west. There is a seasonal shift in the mean snowfall trajectories. In summer, the air parcels originate on average more from the south and east, while in winter mostly from the north, and in autumn and spring mostly from the west. The annual variations in potential moisture source region are a function of variations in strength and tracks of cyclones, in the extent of sea ice, in altitude of the parcels, and in stability of the atmosphere. Assuming the air parcels are close enough to the surface to interact with the surface, we define the location of the air parcels 4 days before arrival as an indicator of the main potential source region. Trends in this location will then represent a trend in source region. The temporal variability in moisture source region is on the order of 3° latitude. During the period under consideration (1979–93), a significant trend northward in moisture source region is found for DML05, and a significant trend southward for Dome C.

If the assumption is made that the spread in air parcel locations 4 days before arrival at level 4 is representative

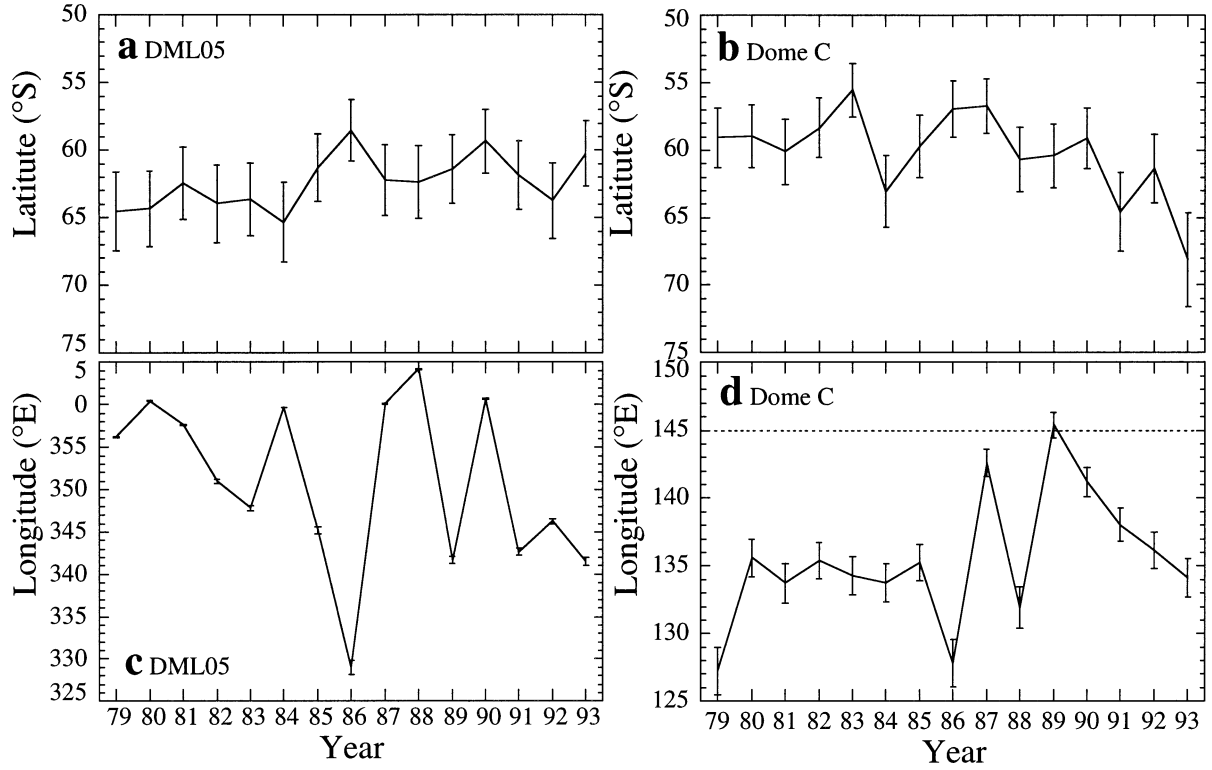

FIG. 12. Annual mean (a), (b) latitude and (c), (d) longitude position of trajectories 4 days before arrival at level 4 at (a), (c) DML05 and (b), (d) Dome C. The error bars denote 1 std dev from the mean.

for the source region distribution, we conclude that moisture sources for precipitation are generally located between 50° and 60°S in the ocean closest to the arrival point. This region contributes ~30% to the total annual precipitation. Previous estimates of the source regions of Antarctic snow scatter considerably, from 8°–40°S (Peixoto and Oort 1992) to 55°–60°S (Delmotte et al. 2000). Our results clearly support the more southerly origin. Owing to the cyclonic curvature of the trajectories and the westerly flow at ~50°S this result holds even when the day-4 assumption is incorrect. The latitude band 40°–70°S, which is the area north of the sea-ice edge, contributes ~75%. The sea surface temperatures in this latitude band range between 0° and 20°C. This results in a main contribution of the Atlantic Ocean for precipitation at DML05 (55%–65%); the Indian Ocean at Dome F (45%–65%), Vostok (30%–45%), and Dome C (60%–75%); and the Pacific Ocean at Byrd (65%–75%). The trajectories show seasonal dependency, resulting in a seasonal cycle in the moisture sources. The seasonal cycle is enhanced by that in the precipitation. Due to the cyclonic curvature of the trajectories the systematic error in the atmospheric circulation in the model due to a faulty elevation of Vostok station (Bromwich et al. 2000) will not change the results significantly.

The snowfall trajectories arriving at Vostok pass over Dome C 12 h before arrival. This partly explains the correlation between precipitation at Dome C and Vostok. The potential source region for precipitation at Vostok is south of the source region of Dome C, although some overlap is present. Therefore, the ice core records are also likely to show similarities, assuming that the general circulation patterns and resulting snowfall trajectories remained reasonably constant over time and the error in the atmospheric circulation in the model reported by Bromwich et al. (2000) will not have a major impact on the calculated trajectories. Note that the results presented here are based on the present-day climate. No attempt has yet been made to extend the results to past climates.

Acknowledgments. We would like to thank Peter Siegmund, Erik van Meijgaard, and Nicole van Lipzig from the KNMI for their help with the trajectory model. D. Bromwich and an unknown reviewer are thanked for the useful comments. Wind data were provided by the ECMWF. This work is a contribution to the European Project for Ice Coring in Antarctica (EPICA), a joint ESF (European Science Foundation)/EC scientific programme, funded by the European Commission under the Environment and Climate Programme (1994–1998) Contract ENV4-CT95-0074 and by national contributions from Belgium, Denmark, France, Germany, Italy, the Netherlands, Norway, Sweden, Switzerland, and the United Kingdom.

REFERENCES

Bromwich, D. H., 1988: Snowfall in high southern latitudes. *Rev. Geophys.,* **26,** 149–168.

——, and C. J. Weaver, 1983: Latitudinal displacement from main moisture source controls $\delta^{18}O$ of snow in coastal Antarctica. *Nature,* **301,** 145–147.

——, A. N. Rogers, P. Kållberg, R. I. Cullather, J. W. C. White, and K. J. Kreutz, 2000: ECMWF analyses and reanalyses depiction of ENSO signal in Antarctic precipitation. *J. Climate,* **13,** 1406–1420.

Ciais, P., J. W. C. White, J. Jouzel, and J. R. Petit, 1995: The origin of present-day Antarctic precipitation from surface deuterium excess data. *J. Geophys. Res.,* **100** (D9), 18 917–18 927.

Cullather, R., D. Bromwich, and R. Grumbine, 1997: Validation of operational numerical analyses in Antarctic latitudes. *J. Geophys. Res.,* **102** (D12), 13 761–13 784.

——, ——, and M. van Woert, 1998: Spatial and temporal variability of Antarctic precipitation from atmospheric methods. *J. Climate,* **11,** 334–367.

Delaygue, G., V. Masson, J. Jouzel, R. D. Koster, and R. J. Healy, 2000: The origin of Antarctic precipitation: A modelling approach. *Tellus,* **52B,** 19–36.

Delmotte, M., V. Masson, and J. Jouzel, 2000: A seasonal deuterium excess signal at Law Dome, coastal eastern Antarctica: A southern ocean signature. *J. Geophys. Res.,* **105** (D6), 7187–7197.

Dome-F Ice Core Research Group, 1998a: Deep ice-core drilling at Dome Fuji and glaciological studies in East Dronning Maud Land, Antarctica. *Ann. Glaciol.,* **27,** 333–337.

——, 1998b: Preliminary investigation of palaeoclimate signals recorded in the ice core from Dome Fuji station, East Dronning Maud Land, Antarctica. *Ann. Glaciol.,* **27,** 338–342.

Doty, K. G., and D. J. Perkey, 1993: Sensitivity of trajectory calculations to the temporal frequency of wind data. *Mon. Wea. Rev.,* **121,** 387–401.

Genthon, C., and A. Braun, 1995: ECMWF analysis and predictions of the surface climate of Greenland and Antarctica. *J. Climate,* **8,** 2324–2332.

Gibson, J. K., P. Kållberg, S. Uppala, A. Hernandez, A. Nomura, and E. Serrano, 1997: ERA-15 description. ECMWF Reanalysis Project Report Series, No. 1, 72 pp.

Giovinetto, M. B., and C. R. Bentley, 1985: Surface balance in ice drainage systems of Antarctica. *Antarct. J. U.S.,* **20** (4), 6–13.

GRIP Members, 1993: Climate instability during the last interglacial period recorded in the GRIP ice core. *Nature,* **364,** 203–207.

Herron, M. M., 1982: Impurity sources of F^-, Cl^-, NO_3^- and SO_4^{2-} in Greenland and Antarctic precipitation. *J. Geophys. Res.,* **87** (C4), 3052–3060.

Jouzel, J., and Coauthors, 1997: Validity of the temperature reconstruction from water isotopes in ice cores. *J. Geophys. Res.,* **102** (C12), 26 471–26 487.

Kahl, J. D., J. M. Harris, and G. A. Herbert, 1989: Intercomparison of three long-range trajectory models applied to Arctic haze. *Tellus,* **41B,** 524–536.

King, J. C., and J. Turner, 1997: *Antarctic Meteorology and Climatology*. Cambridge University Press, 409 pp.

Kottmeier, C., and B. Fay, 1998: Trajectories in the Antarctic lower troposphere. *J. Geophys. Res.,* **103** (D9), 10 947–10 959.

Legrand, M., and R. J. Delmas, 1987: A 220-year continuous record of vulcanic H_2SO_4 in the Antarctic ice sheet. *Nature,* **327,** 671–676.

Noone, D., J. Turner, and R. Mulvaney, 1999: Atmospheric signals and characteristics of accumulation in Dronning Maud Land, Antarctica. *J. Geophys. Res.,* **104** (D16), 19 191–19 212.

Oerter, H., F. Wilhelms, F. Jung-Rothenhäusler, F. Göktas, H. Miller, W. Graf, and S. Sommer, 2000: Accumulation rates in Dronning Maud Land, Antarctica, as revealed by dielectric-profiling measurements at shallow firn cores. *Ann. Glaciol.,* **30,** 27–34.

Peixoto, J. P., and A. H. Oort, 1992: *Physics of Climate*. American Institute of Physics, 520 pp.

Petit, J. R., J. Jouzel, M. Pourchet, and L. Merlivat, 1982: A detailed study of snow accumulation and stable isotope content in Dome C (Antarctica). *J. Geophys. Res.,* **87** (C6), 4301–4308.

——, J. W. C. White, N. W. Young, J. Jouzel, and Y. S. Korotkevich, 1991: Deuterium excess in recent Antarctic snow. *J. Geophys. Res.,* **96** (D3), 5113–5122.

——, and Coauthors, 1999: Climate and atmospheric history of the past 420,000 years from the Vostok ice core, Antarctica. *Nature,* **399,** 429–436.

Reijmer, C. H., and M. R. van den Broeke, 2001: Moisture sources of precipitation in Western Dronning Maud Land, Antarctica. *Antarct. Sci.,* **13** (2), 210–220.

Scheele, M. P., P. C. Siegmund, and P. F. J. van Velthoven, 1996: Sensitivity of trajectories to data resolution and its dependence on the starting point: In or outside a tropopause fold. *Meteor. Appl.,* **3,** 267–273.

Schlosser, E., 1999: Effects of seasonal variability of accumulation on yearly mean $\delta^{18}O$ values in Antarctic snow. *J. Glaciol.,* **45** (151), 463–468.

Stohl, A., G. Wotawa, P. Siebert, and H. Kromp-Kolb, 1995: Interpolation errors in wind fields as a function of spatial and temporal resolution and their impact on different types of kinematic trajectories. *J. Appl. Meteor.,* **34,** 2149–2165.

Turner, J., W. M. Connelley, S. Leonard, G. J. Marshall, and D. G. Vaughan, 1999: Spatial and temporal variability of net snow accumulation over the Antarctic from ECMWF reanalysis project data. *Int. J. Climatol.,* **19,** 697–724.

van den Broeke, M. R., 1997: Spatial and temporal variation of sublimation on Antarctica: Results of a high-resolution general circulation model. *J. Geophys. Res.,* **102** (D25), 29 765–29 777.

Wolff, E., I. Basile, J. Petit, and J. Schwander, 1999: Comparison of Holocene electrical records from Dome C and Vostok, Antarctica. *Ann. Glaciol.,* **29,** 89–93.